Journal of Radioanalytical and Nuclear Chemistry (2019) 320:145–152
https://doi.org/10.1007/s10967-019-06423-x

Extension of experimental activation cross-sections database of deuteron induced nuclear reactions on manganese up to 50 MeV

F. Tárkányi[1] · F. Ditrói[1] · S. Takács[1] · A. Hermanne[2] · A. V. Ignatyuk[3]

Received: 21 November 2018 / Published online: 18 February 2019

Abstract

In the frame of a systematic study of activation cross sections of deuteron induced reactions, experimental cross section data were measured on Mn (monoisotopic ^{55}Mn) up to 50 MeV for the formation of ^{56,54,52}Mn, ^{48}V and ^{51}Cr by using stacked-foil activation method and high resolution gamma spectrometry. The experimental data are compared with the earlier published data and with the results predicted by the ALICE-IPPE-D and EMPIRE-II-D theoretical codes, and with the data taken from the on-line TENDL-2017 library.

Keywords Deuteron irradiation · Off-line gamma spectrometry · Cross section · Mn, V and Cr radioisotopes · Physical yield · Theoretical model codes

Introduction

Activation cross sections of residual nuclides with deuteron are basic data for applications around modern accelerators e.g. in radiation dose estimations for accelerator and target technology, in medical isotope production, in radio-analytical studies for biomedical research and wear control by thin layer activation technique. The status of experimental database for deuteron induced reactions—opposite to protons- is very poor (especially above 15 MeV), no systematical study has been performed earlier and in the published data (except for a few well measured monitor and medically important reactions) show large discrepancies. We hence performed a systematic experimental study of deuteron induced activation cross sections for around 60 elements during the last decades. A systematic comparison with the theoretical models allows conclusions on the predictivity of the different nuclear reaction model codes (ALICE-IPPE, EMPIRE-II, GNASH, TALYS, PHITS).

Manganese metal is an important component of different alloys used in nuclear technology. The experimental activation cross sections data are important for further development of the theoretical codes for deuteron induced nuclear reactions and for optimization of production routes of some medically relevant radionuclides ^{52g}Mn [1] and ^{51}Cr [2].

In spite of the scientific and practical interest, only a couple of authors published cross section data on deuteron induced reactions on Mn. Gilly et al. [3], Baron et al. [4] and Coetzee et al. [5] studied the excitation functions of (*d*, *p*) reactions up to 12 MeV. Ochiai et al. [6] measured the cross section of the activation product ^{54}Mn at 39.5 MeV and our group investigated the excitation functions for the production of ^{56,54,52}Mn and ^{51}Cr (Ditroi et al. [7]).

Thick target yields data were reported by Bondarenko and Rudenko [8] using 3 MeV deuterons for activation analysis; Vakilova et al. [9] also investigated the production yield for the determination of trace elements by deuteron activation. Dmitriev et al. [10] made a systematic study of thick target yields at 22 MeV deuterons induced reactions on a large number of target elements.

In the present work we determined the production cross-section of ^{56,54,52}Mn, ^{48}V and ^{51}Cr in the 50 MeV deuteron induced activation of ^{55}Mn. This has been done to extend the ^{55}Mn(*d*, *x*) reaction cross-sections up to the deuteron energy of 50 MeV.

✉ F. Ditrói
ditroi@atomki.mta.hu

1 Institute of Nuclear Research of the Hungarian Academy of Sciences (ATOMKI), Debrecen, Hungary

2 Cyclotron Laboratory, Vrije Universiteit Brussel (VUB), Brussels, Belgium

3 Institute of Physics and Power Engineering (IPPE), Obninsk, Russia

Experiment and data evaluation

For the cross section determination an activation method, based on stacked foil irradiation followed by γ-ray spectrometry was used. The stack consisted of a sequence of 7 blocks of Hf (10.54 µm), Al (49.54 µm), Al (49.54 µm), Pt (19.29 µm), Al (49.54 µm), Al (49.54 µm), NiMnCu alloy (24.73 µm), Al (49.54 µm), Al (49.54 µm) foils, repeated seven times and bombarded for 3600 s with a 50 MeV proton beam of 100 nA at Louvain la Neuve cyclotron laboratory. The activity produced in the targets and monitor foils was measured non-destructively (without chemical separation) using a high resolution HPGe gamma-ray spectrometer. The evaluation of the gamma-ray spectra was made by both a commercial and an interactive peak fitting codes.

The decay data were taken from the online database NuDat2 [11] and the Q-values of the contributing reactions from the Q-value calculator [12].

The effective beam energy and the energy scale were determined initially by a stopping calculation and finally corrected on the basis of the excitation functions of the ^{24}Al(p, x)^{22,24}Na monitor reactions simultaneously re-measured over the whole energy range. For estimation of the uncertainty of the median energy in the target samples and in the monitor foils, the cumulative errors influencing the calculated energy (incident proton energy, thickness of the foils, beam straggling) have been taken into account. The beam intensity was obtained on the basis of the excitation functions of the monitor reactions. The uncertainty on each cross-section was estimated by taking the square root of the sum in quadrature of all individual contributions.

The important experimental parameters and the methods of data evaluation for this work are summarized in Table 1. The targets consisted of a Ni–Mn–Cu alloy with known composition (Ni: 2%—Mn: 12%—Cu: 86%) and in principle the investigated products (^{56,54,52}Mn, ^{48}V and ^{51}Cr) could, apart from reactions on ^{55}Mn, also be produced by nuclear reactions on the other two alloy components. The cross sections for activation of these product nuclides on Ni and Cu by deuterons were, however, investigated by us earlier [13, 14]. Based on the published results and on the target composition we only had to introduce negligible corrections to the

Table 1 Important parameters of the experiments and methods of data evaluations

Experiment		Data evaluation	
Incident particle	Proton	Gamma spectra evaluation	Genie 2000 [15], Forgamma [16]
Method	Stacked foil	Determination of beam intensity	Faraday cup (preliminary) Fitted monitor reaction (final) [17]
Target stack and thicknesses	7 blocks of Hf (10.54 µm), Al (49.54 µm), Al (49.54 µm), Pt(19.29 µm), Al (49.54 µm), Al (49.54 µm), Ni(2) Mn(12)Cu(86) alloy (24.73 µm), Al (49.54 µm), Al (49.54 µm)	Decay data	NUDAT 2.7 [18]
Number of target foils	7/group	Reaction Q-values	Q-value calculator [12]
Accelerator	Cyclone 90 cyclotron of Université Catholique in Louvain la Neuve (LLN) Belgium	Determination of beam energy	Andersen-Ziegler (preliminary) [19] Fitted monitor reaction (final) [20]
Primary energy	50 MeV	Uncertainty of energy	Cumulative effects of possible uncertainties
Irradiation time	60 min	Cross sections	Isotopic cross section
Beam current	100 nA	Uncertainty of cross sections	Sum in quadrature of all individual contributions [21]
Monitor reaction, [recommended values]	^{27}Al(d, x)^{22,24}Na [20]	Yield	Physical yield [22, 23]
Monitor target and thickness	Al (49.54 µm)	Theory	ALICE-IPPE-D [24], EMPIRE-II-D [25], TALYS 1.9 in (TENDL-2017) [26]
Detector	HPGe		
γ-spectra measurements	4 series		
Cooling times (h)	8.9–11.0 48.1–71.9 199.3–319.6 3167.1–3671.2		

cross sections derived in the present study. The decay data used are presented in Table 2.

Theoretical calculations od cross sections

The results for model calculations, performed up to 50 MeV, are taken from our previous study [7]. The updated ALICE-IPPE-D [24] and EMPIRE-D [25] codes were used to compare with the experimental results. As described in detail in Tarkanyi et al. [27] and Hermanne et al. [28] these improved codes were developed to achieve a better description of deuteron induced reactions. In the original versions of the programs a simulation of direct (*d*, *p*) and (*d*, *t*) phenomena is applied through an energy dependent enhancement factor for the transitions in question. The selection of parameters is given in [29]. The theoretical data from the recently updated TENDL-2017 [30] library (based on the modified TALYS 1.9 code [31]) was also used for a comparison.

Cross sections

The cross sections for reactions studied are shown in Figs. 1, 2, 3, 4 and 5 and the numerical values are collected in Table 3.

^{55}Mn(*d, p*)^{56}Mn reaction

The excitation function for ^{56}Mn ($T_{1/2}$ = 2.5789 h) radioisotope, formed by the ^{55}Mn(*d*, *p*)^{56}Mn reaction, is shown in Fig. 1, together with the previous experimental data and theoretical calculations. The agreement of our new data with the literature values in the studied energy range is acceptable. When comparing all experimental data with the results

Table 2 Decay characteristics of the activation products

Nuclide	Half-life	E_γ keV)	I_γ (%)	Contributing reaction	*Q*-value (keV)
^{56}Mn	2.5789 h	846.7638	98.85	^{55}Mn(*d*, *p*)	5045.884
		1810.726	26.9		
^{54}Mn	312.20 d	834.848	99.976	^{55}Mn(*d*, *p2n*)	−12,451.09
^{52}Mn	5.591 d	744.233	90.0	^{55}Mn(*d*,*p*4*n*)	−33,443.66
		935.544	94.5	^{52}Fe decay	−36,599.83
		1434.092	100.0		
^{51}Cr	27.7025 d	320.0824	9.91	^{55}Mn(*d*, 2*p*4*n*)	−39,989.27
^{48}V	15.9735 d	983.525	99.98	^{55}Mn(*d*, 3*p*6*n*)	−70,393.83
		1312.106	98.2	^{48}Cr decay	−72,831.86

Modify *Q*-values for emission of clustered particles with: $pn \rightarrow d$ +2.2 MeV, $p2n \rightarrow t$ +8.5 MeV, $2pn \rightarrow {}^3$He +7.7 MeV, $2p2n \rightarrow \alpha$ +28.3 MeV

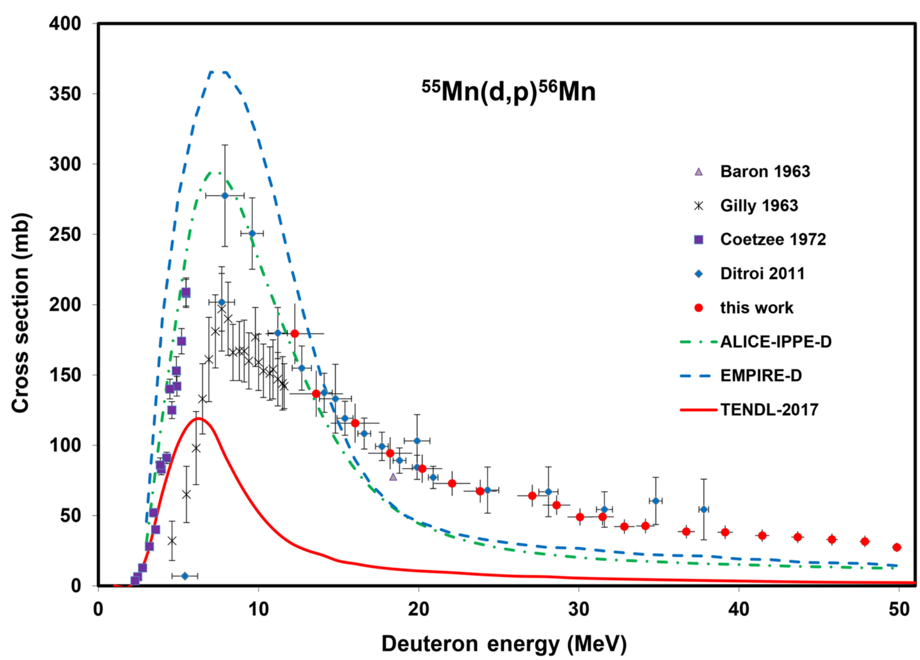

Fig. 1 Experimental and theoretical excitation functions for the ^{55}Mn(*d*, *p*)^{56}Mn reaction

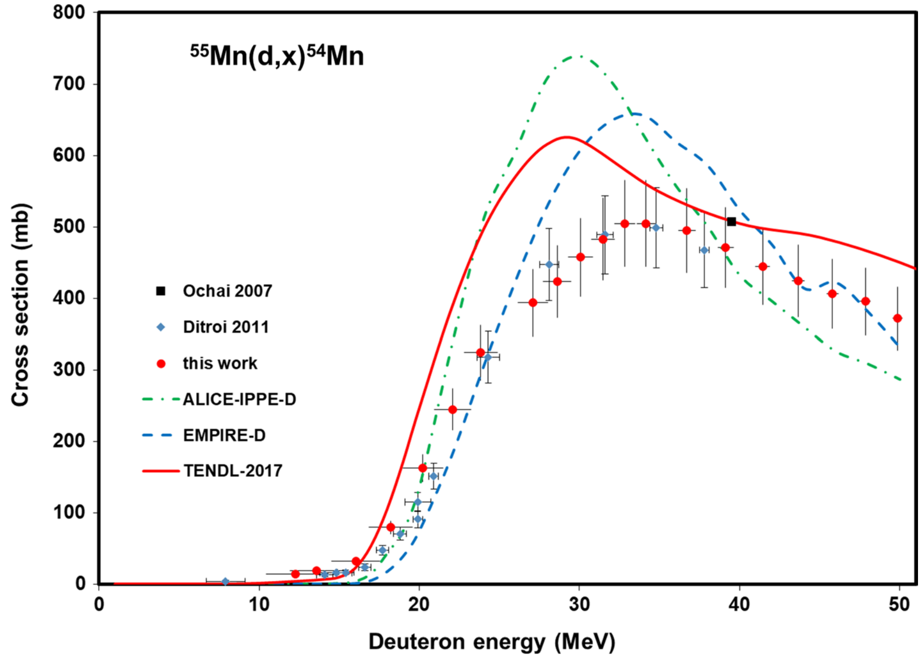

Fig. 2 Experimental and theoretical excitation functions for the ^{55}Mn(d, x)^{54}Mn reaction

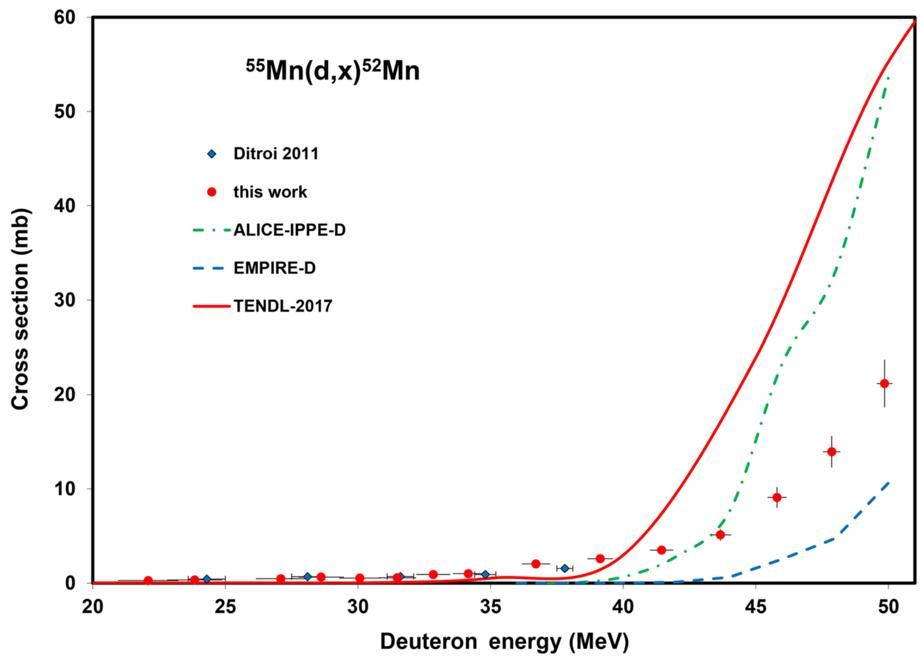

Fig. 3 Experimental and theoretical excitation functions for the ^{55}Mn(d, x)^{52g}Mn cumulative reaction

of theoretical calculations the agreement is good in case of ALICE-IPPE-D and EMPIRE-D up to 15 MeV but above this energy the theoretical values decrease faster. A significant difference in the magnitude of the cross sections is observed for TENDL-2017.

^{55}Mn(d, x)^{54}Mn reaction

For production of ^{54}Mn ($T_{1/2} = 312.20$ days) the previously published single data point of Ochiai et al. [6] and our earlier data [7] are in good agreement with the new results (Fig. 2). The theoretical descriptions are acceptable regarding the shape, but the overestimation is significant especially around the maximum. The best agreement can be observed with the EMPIRE-D up to 25 MeV and above 40 MeV. The maximum energy of the excitation function curve is estimated almost correctly by the EMPIRE-D.

Fig. 4 Experimental and theoretical excitation functions for the ^{55}Mn(*d*, *x*)^{51}Cr reaction

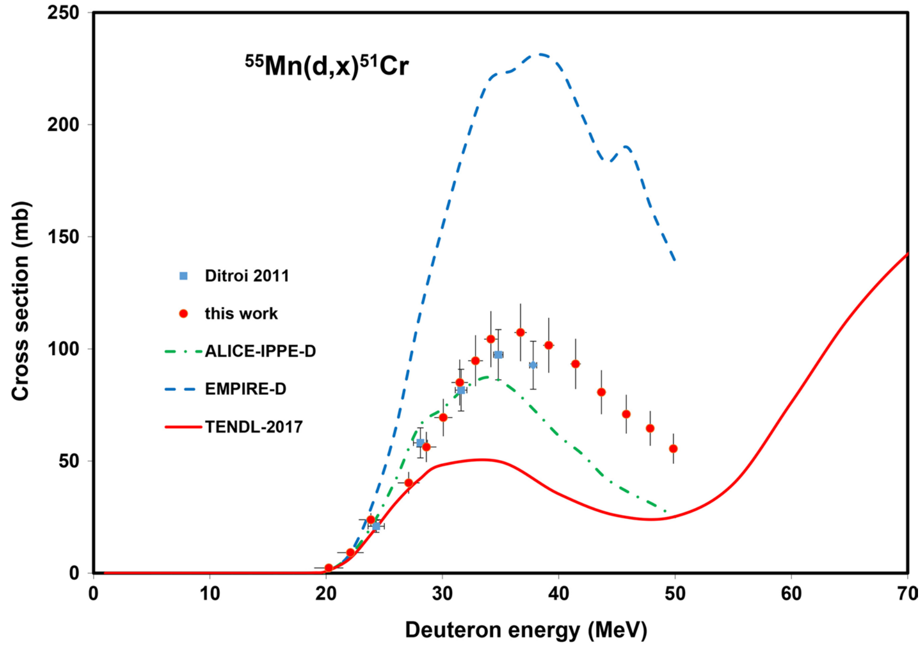

Fig. 5 Experimental and theoretical excitation functions for the ^{55}Mn(*d*, *x*)^{48}V reaction

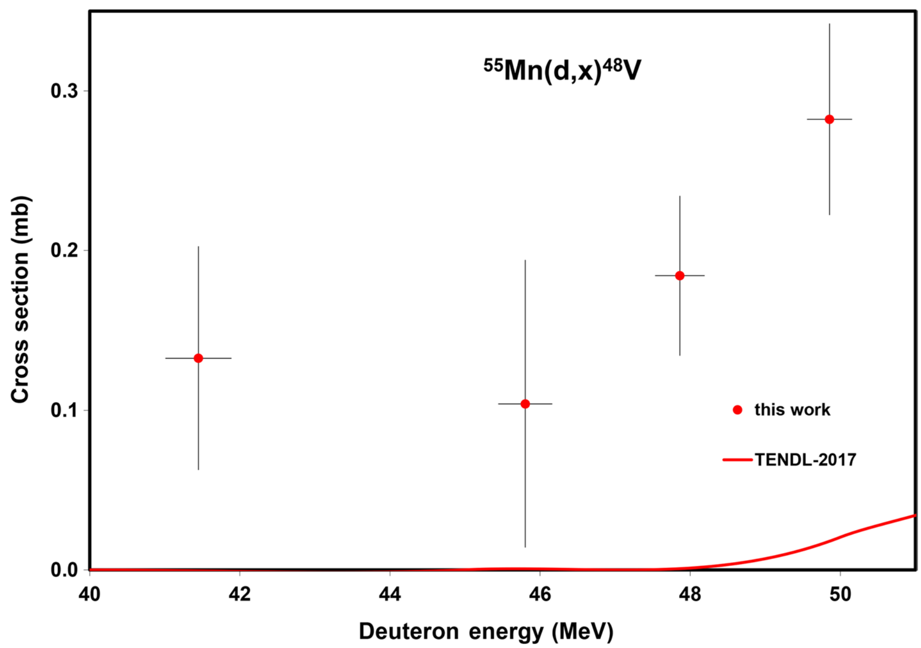

^{55}Mn(*d*, *x*)^{52}Mn reaction

The long-lived radionuclide ^{52}Mn ($T_{1/2}$ = 5.591 days for the ground state) is produced via the reaction ^{55}Mn(*d*, *p*4*n*) with high threshold and through the decay of shorter-lived parent ^{52}Fe ($T_{1/2}$ = 8.725 h, Q = 37.9 MeV). We could not identify the gamma-lines of ^{52}Fe in our spectra (E_γ = 168.688 keV, I_γ = 99.2%), but the presented cross section values are cumulative and include also the small contribution by isomeric decay (1.75%) of the short-lived metastable state ^{52m}Mn. The data of the different theoretical codes show large differences (Fig. 3), ALICE and above 45 MeV and EMPIRE underestimates in the same energy range.

^{55}Mn(*d*, *x*)^{51}Cr reaction

The practical threshold around 20 MeV indicates that the main contributing process for production of ^{51}Cr (27.701 days) is the ^{55}Mn(*d*, α2*n*) reaction and that contributions of the high threshold, short half-life, ^{51}Fe–^{51}Mn decay chain is negligible. The new data are in good agreement with our previous lower energy data (Fig. 4). There are large

Table 3 Production cross sections of deuteron induced reactions on manganese

Energy (MeV)	^{56}Mn (mbarn)	^{54}Mn (mbarn)	^{52}Mn (mbarn)	^{51}Cr (mbarn)	^{48}V (mbarn)
49.9 ± 0.3	27.4 ± 3.3	371.6 ± 44.4	21.2 ± 2.5	55.5 ± 6.7	0.28 ± 0.06
47.9 ± 0.3	31.6 ± 4.1	395.5 ± 47.2	13.9 ± 1.7	64.6 ± 7.8	0.18 ± 0.05
45.8 ± 0.4	33.0 ± 4.3	406.6 ± 48.6	9.1 ± 1.1	70.9 ± 8.7	0.1 ± 0.09
43.7 ± 0.4	34.7 ± 4.2	424.5 ± 50.7	5.1 ± 0.6	80.7 ± 9.8	
41.5 ± 0.4	35.8 ± 4.4	444.3 ± 53.0	3.5 ± 0.4	93.3 ± 11.2	0.13 ± 0.07
39.1 ± 0.5	38.1 ± 4.8	471.2 ± 56.3	2.6 ± 0.3	101.6 ± 12.2	
36.7 ± 0.5	38.5 ± 4.8	495.2 ± 59.1	2.0 ± 0.3	107.3 ± 12.9	
34.2 ± 0.6	42.6 ± 5.2	504.7 ± 60.2	1.01 ± 0.13	104.3 ± 12.5	
32.8 ± 0.6	42.1 ± 5.2	504.9 ± 60.3	0.92 ± 0.13	94.7 ± 11.4	
31.5 ± 0.7	49.1 ± 6.0	482.7 ± 57.6	0.57 ± 0.10	85.0 ± 10.2	
30.1 ± 0.8	49. ± 6.0	457.6 ± 54.7	0.54 ± 0.09	69.4 ± 8.4	
28.6 ± 0.9	57.4 ± 7.0	423.5 ± 50.5	0.64 ± 0.08	56.3 ± 6.7	
27.1 ± 0.9	64.1 ± 7.8	393.6 ± 47.0	0.47 ± 0.07	40.3 ± 4.9	
23.8 ± 1.0	67.3 ± 8.2	324.1 ± 38.7	0.34 ± 0.05	23.8 ± 2.9	
22.1 ± 1.1	72.8 ± 8.8	244.6 ± 29.2	0.27 ± 0.03	9.2 ± 1.1	
20.2 ± 1.3	83.4 ± 10.1	162.6 ± 19.5			
18.2 ± 1.4	94.3 ± 11.4	79.3 ± 9.5			
16.0 ± 1.5	115.7 ± 13.9	32.4 ± 4.0			
13.6 ± 1.7	136.6 ± 16.4	18.6 ± 2.4			
12.3 ± 1.8	179.3 ± 21.5	14.1 ± 1.8			

disagreements between the different theoretical predictions and consequently with the experimental data. Only ALICE-D produces partial agreement up to 35 MeV.

^{55}Mn(*d*, *x*)^{48}V reaction

We obtained only a few cross section data points for production of ^{48}V ($T_{1/2}$ = 15.9735 days) through clustered emission near the reaction threshold (Fig. 5). The data points could only be measured with relatively large errors. Comparable theoretical predictions could only be found in the TENDL-2017 on-line library and this calculation strongly underestimates the experimental data.

Thick target yields

Thick target yields (integral yields for a given bombarding energy down to the threshold of the reaction) were calculated for ^{56,54,52}Mn and ^{51}Cr from fitted curves to our experimental cross section data The results for physical yields [22, 23] are presented in Fig. 6.

Summary

Excitation functions for the production of ^{56,54,52}Mn, ^{51}Cr and ^{48}V by deuteron irradiation of monoisotopic manganese targets were determined. Out of the investigated reactions no earlier data were available for ^{48}V while for ^{54,52}Mn and ^{51}Cr practically only our recently measured and published experimental data exists showing good agreement in the overlapping energy range. For the production of ^{56}Mn, more earlier experimental data are available, which show only moderate agreement with our new results. Comparison of our experimental results with the predictions of theoretical codes show rather variable agreement. The disagreement is very significant in some cases.

Concerning the possible applications, manganese is a significant alloying element for different iron containing end even iron-free alloys. Knowledge of the deuteron-induced activation cross sections up to higher energies is important for improvement of recommended data for different activation data libraries: for Fusion Evaluated Nuclear Library [32], for JANIS Book of deuteron-induced cross-sections [33, 34] and for European Activation File [35] for calculation of induced activity for the high intensity deuteron accelerators (IFMIF [34, 36] Spiral [37] and other accelerator driven neutron sources [38]).

Acknowledgements Open access funding provided by MTA Institute for Nuclear Research (MTA ATOMKI). The authors of this paper acknowledge the support of the participating institutions and

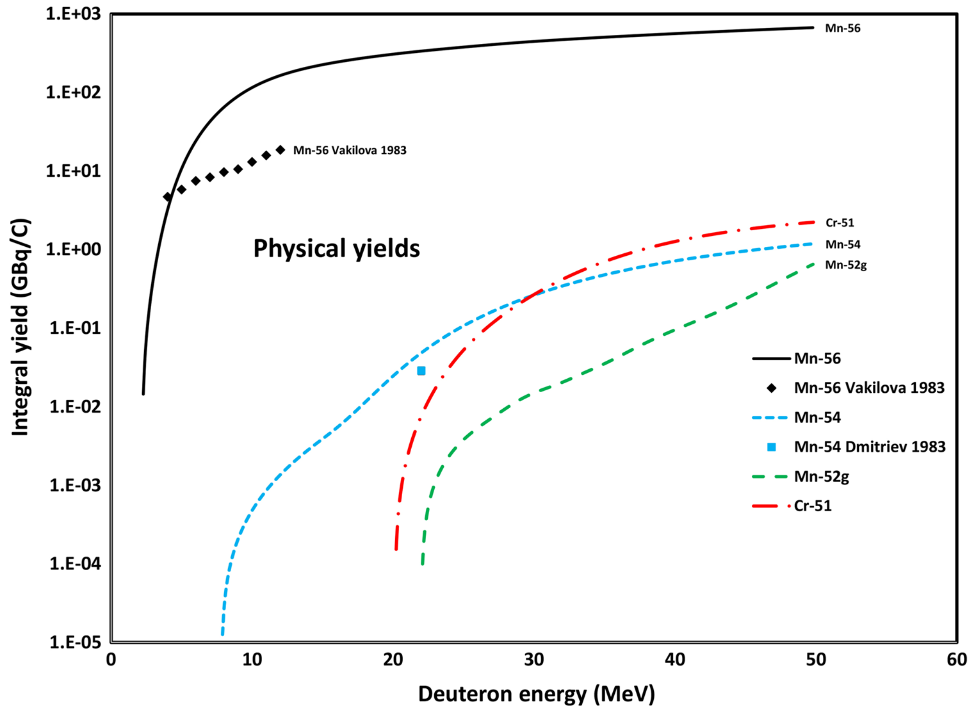

Fig. 6 Integral yields for production of ^{56,54,52}Mn and ^{51}Cr deduced from the excitation functions

the accelerator staffs for providing the beam time and experimental facilities.

References

1. Coenen HH, Buchholz M, Spahn I (2014) Production of 52gMn and 147Gd for the development of multi-modal imaging probes. Nucl Med Biol 41(7):646. https://doi.org/10.1016/j.nucmedbio.2014.05.076
2. Rand ML, Packham MA, Mustard JF (1983) Survival of density subpopulations of rabbit platelets: use of 51Cr-or 111In-labeled platelets to measure survival of least dense and most dense platelets concurrently. Blood 61(2):362–367
3. Gilly LJ, Henriet GA, Alves MP, Capron PC (1963) Absolute cross sections and excitation functions for (*d*, *p*) and (*d*, 2*n*) reactions on ^{55}Mn, ^{63}Cu, ^{65}Cu, ^{66}Zn, and ^{68}Zn between 3 and 11.6 MeV. Phys Rev 131(4):1727–1731. https://doi.org/10.1103/physrev.131.1727
4. Baron N, Cohen BL (1963) Activation cross-section survey of deuteron-induced reactions. Phys Rev 129(6):2636–2642
5. Coetzee Paul P, Peisach M (1972) Activation cross sections for deuteron-induced reactions on some elements of the first transition series, up to 5.5 MeV. Radiochim Acta. https://doi.org/10.1524/ract.1972.17.1.1
6. Ochiai K, Nakao M, Kubota N, Sato S, Yamauchi M, Ishioka NH, Nishitani T, Konno C (2007) Deuteron induced activation cross section measurement for IFMIF. In: Conf. on Nucl. Data for Sci. And Technology, Nice, France, 2007. p 1011
7. Ditrói F, Tárkányi F, Takács S, Hermanne A, Yamazaki H, Baba M, Mohammadi A, Ignatyuk AV (2011) Activation cross-sections of deuteron induced nuclear reactions on manganese up to 40 MeV. Nucl Instrum Methods Phys Res Sect B 269(17):1878–1883. https://doi.org/10.1016/j.nimb.2011.05.020
8. Bondarenko YI, Rudenko VS (1982) Use of deuterons with 3-Mev energy in activation-analysis. At Energy (NY, NY, US) 52(3):193–194. https://doi.org/10.1007/Bf01126994
9. Vakilova G, Vasidov A, Mukhammedov S, Pardaev E, Rakhmanov A, Saidmuradov Z (1983) Sensitivity of the determination of some elements with Z less-than-or-equal-to 42 by a deuteron activational method in a cyclotron. At Energy (NY, NY, US) 55(3):598–602. https://doi.org/10.1007/Bf01127995
10. Dmitriev PP, Krasnov NN, Molin GA (1982) Radioactive nuclide yields for thick target at 22 MeV deuterons energy. Yadernie Konstanti 34(4):38
11. NuDat2 database (2.6) (2014) National Nuclear Data Center, Brookhaven National Laboratory. http://www.nndc.bnl.gov/nudat2/
12. Q-value calculator (2003) NNDC, Brookhaven National Laboratory. http://www.nndc.bnl.gov/qcalc
13. Takács S, Tárkányi F, Király B, Hermanne A, Sonck M (2007) Evaluated activation cross sections of longer-lived radionuclides produced by deuteron induced reactions on natural nickel. Nucl Instrum Methods Phys Res Sect B 260(2):495–507. https://doi.org/10.1016/j.nimb.2006.11.136
14. Takács S, Tárkányi F, Király B, Hermanne A, Sonck M (2006) Evaluated activation cross sections of longer-lived radionuclides produced by deuteron-induced reactions on natural copper. Nucl Instrum Methods Phys Res Sect B 251(1):56–65. https://doi.org/10.1016/j.nimb.2006.06.007
15. Canberra (2000) http://www.canberra.com/products/radiochemistry_lab/genie-2000-software.asp. 2013

16. Székely G (1985) Fgm—a flexible gamma-spectrum analysis program for a small computer. Comput Phys Commun 34(3):313–324. https://doi.org/10.1016/0010-4655(85)90008-6
17. Tárkányi F, Szelecsényi F, Takács S (1991) Determination of effective bombarding energies and fluxes using improved stacked-foil technique. Acta Radiol Suppl 376:72
18. Kinsey RR, Dunford CL, Tuli JK, Burrows TW (1997) in Capture gamma-ray spectroscopy and related topics, vol 2. (NUDAT 2.6 http://www.nndc.bnl.gov/nudat2/), vol 2. Springer Hungarica Ltd, Budapest
19. Andersen HH, Ziegler JF (1977) Hydrogen stopping powers and ranges in all elements. The stopping and ranges of ions in matter, vol 3. The Stopping and ranges of ions in matter, vol 3. Pergamon Press, New York
20. Tárkányi F, Takács S, Gul K, Hermanne A, Mustafa MG, Nortier M, Oblozinsky P, Qaim SM, Scholten B, Shubin YN, Youxiang Z (2001) Beam monitor reactions (Chapter 4). Charged particle cross-section database for medical radioisotope production: diagnostic radioisotopes and monitor reactions. TECDOC 1211, vol 1211. IAEA
21. International-Bureau-of-Weights-and-Measures (1993) Guide to the expression of uncertainty in measurement, 1st edn. International Organization for Standardization, Genève
22. Bonardi M (1987) The contribution to nuclear data for biomedical radioisotope production from the Milan cyclotron facility. In: Paper presented at the consultants meeting on data requirements for medical radioisotope production, Tokyo, Japan
23. Otuka N, Takács S (2015) Definitions of radioisotope thick target yields. Radiochim Acta 103(1):1–6. https://doi.org/10.1515/ract-2013-2234
24. Dityuk AI, Konobeyev AY, Lunev VP, Shubin YN (1998) New version of the advanced computer code ALICE-IPPE. INDC (CCP)-410. IAEA, Vienna
25. Herman M, Capote R, Carlson BV, Oblozinsky P, Sin M, Trkov A, Wienke H, Zerkin V (2007) EMPIRE: nuclear reaction model code system for data evaluation. Nucl Data Sheets 108(12):2655–2715. https://doi.org/10.1016/j.nds.2007.11.003
26. Koning AJ, Rochman D, Kopecky J, Sublet JC, Bauge E, Hilaire S, Romain P, Morillon B, Duarte H, van der Marck S, Pomp S, Sjostrand H, Forrest R, Henriksson H, Cabellos O, S. G, Leppanen J, Leeb H, Plompen A, Mills R (2015) TENDL-2015: TALYS-based evaluated nuclear data library. https://tendl.web.psi.ch/tendl_2015/tendl2015.html
27. Tárkányi F, Hermanne A, Takács S, Hilgers K, Kovalev SF, Ignatyuk AV, Qaim SM (2007) Study of the ^{192}Os(d, 2n) reaction for, production of the therapeutic radionuclide ^{192}Ir in no-carrier added form. Appl Radiat Isot 65(11):1215–1220. https://doi.org/10.1016/j.apradiso.2007.06.007
28. Hermanne A, Tárkányi F, Takács S, Ditrói F, Baba M, Ohtshuki T, Spahn I, Ignatyuk AV (2009) Excitation functions for production of medically relevant radioisotopes in deuteron irradiations of Pr and Tm targets. Nucl Instrum Methods Phys Res Sect B 267(5):727–736. https://doi.org/10.1016/j.nimb.2008.12.017
29. Belgya T, Bersillon O, Capote R, Fukahori T, Zhigang G, Goriely S, Herman M, Ignatyuk AV, Kailas S, Koning A, Oblozinsky P, Plujko V, Young P (2005) Handbook for calculations of nuclear reaction data: Reference Input Parameter Library. http://www-nds.iaea.org/RIPL-2/. IAEA, Vienna
30. Koning AJ, Rochman D, Sublet JC (2017) TENDL-2017 TALYS-based evaluated nuclear data library. https://tendl.web.psi.ch/tendl_2017/tendl2017.html. 2018
31. Koning AJ, Hilaire S, Duijvestijn MC (2007) TALYS-1.0. In: Paper presented at the international conference on nuclear data for science and technology, Nice, France
32. IAEA (2011) Fusion Evaluated Nuclear Data Library FENDL 3.0. IAEA. http://www-nds.iaea.org/fendl3/. 2013
33. Soppera N, Dupont E, Bossant M, Fleming M (2018) JANIS book of deuteron-induced cross-sections comparison of evaluated and experimental data from ENDF/B-VIII.0, TENDL-2017 and EXFOR. http://www.oecd-nea.org/janis/book/book-deuteron-2018-05.pdf. JANIS Books. OECD NEA Data Bank
34. Blideanu V, García M, Joyer P, López D, Mayoral A, Ogando F, Ortíz F, Sanz J, Sauvan P (2011) Deuteron cross section evaluation for safety and radioprotection calculations of IFMIF/EVEDA accelerator prototype. J Nucl Mater 417(1):1271–1274. https://doi.org/10.1016/j.jnucmat.2010.12.270
35. Forrest RA, Kopecky J (2009) The activation system EASY-2007. J Nucl Mater 386:878–881. https://doi.org/10.1016/j.jnucmat.2008.12.194
36. IFMIF (1996) IFMIF conceptual design activity, final report. IFMIF. http://www.frascati.enea.it/cda/FinalReport/. 2018
37. GANIL (2005) Origin of the SPIRAL2 project. GANIL. http://pro.ganil-spiral2.eu/spiral2/origin-of-spiral2
38. Nagai Y, Hashimoto K, Hatsukawa Y, Saeki H, Motoishi S, Sato N, Kawabata M, Harada H, Kin T, Tsukada K, Sato TK, Minato F, Iwamoto O, Iwamoto N, Seki Y, Yokoyama K, Shiina T, Ohta A, Takeuchi N, Kawauchi Y, Sato N, Yamabayashi H, Adachi Y, Kikuchi Y, Mitsumoto T, Igarashi T (2013) Generation of radioisotopes with accelerator neutrons by deuterons. J Phys Soc Jpn 82(6):4201